Characterization of nitrides by electron paramagnetic resonance (EPR) and optically detected magnetic resonance (ODMR)

E.R. Glaser [a,*], W.E. Carlos [a], G.C.B. Braga [a,1], J.A. Freitas, Jr [a], W.J. Moore [b],
B.V. Shanabrook [a], A.E. Wickenden [a,2], D.D. Koleske [a], R.L. Henry [a], M.W. Bayerl [c,3],
M.S. Brandt [c], H. Obloh [d], P. Kozodoy [e,4], S.P. DenBaars [e], U.K. Mishra [e],
S. Nakamura [e], E. Haus [f], J.S. Speck [f], J.E. Van Nostrand [g], M.A. Sanchez [h],
E. Calleja [h], A.J. Ptak [i], T.H. Myers [i], R.J. Molnar [j]

[a] *Naval Research Laboratory, Washington, DC 20375-5347, USA*
[b] *SFA Inc, Largo, MD 20744, USA*
[c] *Walter Schottky Institut, Technische Universität München, D-85748 Garching, Germany*
[d] *Fraunhofer-Institut für Angewandte Festkörperphysik, D-79108 Freiburg, Germany*
[e] *Electrical and Computer Engineering, College of Engineering, University of California, Santa Barbara, CA 93016, USA*
[f] *Materials Department, College of Engineering, University of California, Santa Barbara, CA 93016, USA*
[g] *Air Force Research Laboratory, Wright-Patterson AFB, OH 45433-7322, USA*
[h] *Department of Electronic Engineering, Polytechnical University of Madrid, 28040 Madrid, Spain*
[i] *Physics Department, West Virginia University, Morgantown, VA, West Virginia, WV 26506, USA*
[j] *Lincoln Laboratory, Massachusetts Institute of Technology, Lexington, MA 02173, USA*

Abstract

We will highlight our recent work on the properties of residual defects and dopants in GaN heteroepitaxial layers and on the nature of recombination from InGaN single quantum well (SQW) light emitting diodes (LEDs) through magnetic resonance techniques. Electron paramagnetic resonance (EPR) and optically detected magnetic resonance (ODMR) were performed on undoped (highly resistive and n-type) and intentionally doped (Si, Mg, or Be) GaN films grown by a variety of techniques (MOCVD, MBE, and HVPE) in order to obtain general trends and behavior. Through the spin-Hamiltonian parameters, these methods can reveal symmetry information, the character of the wave function and (ideally) the chemical identity of the defect. In addition, low temperature EPR intensities can be used to determine the neutral acceptor or donor concentrations without the need for contacts or the high temperatures required for Hall effect measurements. The ODMR was performed on both bandedge (mainly shallow donor–shallow acceptor recombination) and deep (visible and near-IR) PL bands. In spite of the radically different (non-equilibrium) growth techniques, many of the same defects were found in the various samples. Finally, earlier ODMR studies of recombination from Nichia InGaN 'green' and 'blue' LEDs were extended to include shorter ('violet') and longer ('amber') wavelength LEDs and an undoped 30 Å $In_{0.3}Ga_{0.7}N$/GaN heterostructure. The results provide evidence for spatially separated electrons and holes in the optically-active 30 Å InGaN layers under low photoexcitation conditions, likely due to localization at different potential minima in the $x-y$ planes and/or the large strain-induced piezoelectric fields parallel to the growth direction.
© 2002 Elsevier Science B.V. All rights reserved.

Keywords: GaN; InGaN LEDs; p-Type doping; Photoluminescence; Magnetic resonance

* Corresponding author. Tel.: +1-202-404-4521; fax: +1-202-767-1165.
E-mail address: glaser@bloch.nrl.navy.mil (E.R. Glaser).
[1] Permanent address: Physics Institute, Universidade de Brasilia, Brasilia, Brazil.
[2] Present address: Army Research Laboratory, Adelphi, MD 20783-1197 USA.
[3] Present address: Infineon Technologies AG, D-81609 München, Germany.
[4] Present address: Cree Lighting Company, Goleta, CA 93117 USA.

1. Introduction

During the last decade a variety of defect-sensitive spectroscopic tools have been applied to obtain detailed information on the properties of residual defects and dopants in GaN and to learn more about their roles in the recombination processes observed from this technologically important semiconductor system. In particular, magnetic resonance techniques, such as electron paramagnetic resonance (EPR) and optically detected magnetic resonance (ODMR) have been performed by several groups on as-grown and doped GaN heteroepitaxial layers to provide information on the character of the ground and excited defect states, respectively [1,2]. In addition, the nature of the recombination from state-of-the-art InGaN single-quantum-well light emitting diodes (LEDs) has been investigated by ODMR [3]. The defects in the active layers or contact regions that possibly limit performance of such devices have also been explored by electrically detected magnetic resonance (EDMR) [4].

In this paper we will review what has been learned from EPR and ODMR about the character of residual defects and dopants in GaN epitaxial layers grown by metal–organic chemical vapor deposition (MOCVD), molecular beam epitaxy (MBE) and hydride vapor phase epitaxy (HVPE) in order to obtain general trends and behavior. In spite of the radically different growth techniques, many of the same residual and dopant-related defects are observed in the various samples. Examples will also be given where different defects are revealed from ODMR on emission bands that appear at first examination to be quite similar based on their peak energies and linewidths. In addition, earlier ODMR studies [3] of recombination under low pumping conditions from commercial InGaN single quantum well (SQW) LEDs have been extended to include shorter ('violet') and longer ('amber') wavelength device structures. Similar experiments were performed on simple $In_{0.3}Ga_{0.7}N(t = 30$ Å$)$/GaN heterostructures for comparison. The strong ODMR observed in these cases indicate significant charge separation under low photo-excitation, likely due to localization of the electrons and holes at different potential minima in the $x–y$ planes and/or spatial separation along the growth direction (even for such thin InGaN layers) from the large strain-induced piezoelectric fields ($\sim 10^6$ V cm^{-1}).

2. Experimental background

The EPR and ODMR experiments were performed on a variety of undoped (high resistivity and n-type) and intentionally doped (Si, Mg, or Be) GaN epitaxial layers grown by MOCVD, MBE, and HVPE. Most of the films were deposited on sapphire substrates (samples No. 5 and 6 were grown on 6H–SiC and Si, respectively). The MBE films were grown using either ammonia (No. 13) or an rf plasma (Nos. 5–8 and 14) as the source for nitrogen. Additional details are provided elsewhere [5–12]. The electrical properties of the layers were obtained from either room temperature Hall effect (variable-temperature studies were carried out in some cases) or two-point probe measurements. Many of the samples were also characterized by secondary ion mass spectroscopy (SIMS) to determine the concentrations of the various dopants and the levels of common residual impurities such as C, O, Si, and H. The layer thickness and the conductivity type/carrier concentration at 300 K are summarized in Table 1. In addition, ODMR was performed on several NICHIA single-quantum-well InGaN LEDs with peak energies between 2.0 and 3.2 eV [13] and on an undoped 30 Å $In_{0.3}Ga_{0.7}N$/GaN heterostructure.

The EPR was done in a commercial 9.5 GHz spectrometer with the samples rotated in the (1120) planes to obtain symmetry information. P-doped Si was used as a standard to obtain the density of spins associated with the EPR signals. The PL at 1.6 K from the GaN films was excited by the 351-nm line of an Ar$^+$ laser. Lines at either 458 or 364 nm were employed to excite preferentially the emission from the InGaN LEDs and heterostructure. The PL between 1.3 and 3.5 eV was studied by a 1/4 m double-grating spectrometer and detected by either a Si photodiode or a GaAs PMT (high-resolution PL for some of these samples is reported elsewhere [14–16]). The 24 and 35 GHz ODMR spectrometers employed in this work have been described previously [17,18].

3. Results and discussion

3.1. Undoped (highly resistive and n-type) and Si-doped GaN

Representative EPR spectra obtained for two n-type (as-grown and Si-doped) GaN films are shown in the top half of Fig. 1. A single line with axial symmetry about the c-axis is found with $g_{\parallel} = 1.951$ and $g_{\perp} = 1.948$ and a full-width at half-maximum (FWHM) of $\sim 0.5–4.0$ mT. This resonance has been firmly established as a 'fingerprint' for shallow donors/conduction electrons in GaN [19–21]. Similar features were observed for samples No. 1 and 4 (not shown). In addition, the absence of an EPR signal from sample No. 2 is consistent with the high-resistivity character as revealed by two-point probe measurements ($V_{breakdown} > 1000$ V).

Possible candidates for the residual donors in sample No. 2–4 are Si and O. Due to the absence of additional structure in these lines from, for example, electron-

Table 1
Summary of pertinent parameters of the GaN epitaxial layers discussed in this work

Sample designation	Source	Growth technique	Thickness (μm)	Doping (cm^{-3})	Transport properties (300 K) (cm^{-3})
No. 1 (#50209)	NRL	CVD	3.5	None	Highly resistive
No. 2 (GaN #1)	APA Optics	CVD	5.6	None	$n \sim 3 \times 10^{16}$
No. 3 (#LH1059)	MIT/LL	HVPE	10	None	$n \sim 1 \times 10^{17}$
No. 4 (#LH1106)	MIT/LL	HVPE	5	None	$n \sim 1 \times 10^{17}$
No. 5 (#052299A)	UCSB	MBE	1	Si	$n \sim 1 \times 10^{17}$
No. 6 (#173)	U. Madrid	MBE	0.5	Be $(10^{19}-10^{20})$[a]	Highly resistive
No. 7 (#0021)	WVU	MBE	2	Be (3×10^{18})[b]	Highly resistive
No. 8 (#0022)	WVU	MBE	2	Be (3×10^{18})[b]	Highly resistive
No. 9 (#980804)	NRL	CVD	1.5	Mg (2.5×10^{18})[b]	Highly resistive
No. 10 (#2947)	Freiburg	CVD	2.5	Mg (1.4×10^{19})[b]	Highly resistive
No. 11 (#990607)	NRL	CVD	1.6	Mg $(2-4 \times 10^{19})$[b]	$p \sim 1.7 \times 10^{17}$
No. 12 (#990401PB)	UCSB	CVD	1	Mg $(3-4 \times 10^{19})$[b]	$p \sim 2.7 \times 10^{17}$
No. 13 (#A377)	WPAFB	MBE	1	Mg $(3-4 \times 10^{19})$[a]	$p \sim 4.0 \times 10^{17}$
No. 14 (#100499A)	UCSB	MBE	0.4	Mg $(4-5 \times 10^{19})$[a]	$p \sim 9.0 \times 10^{17}$

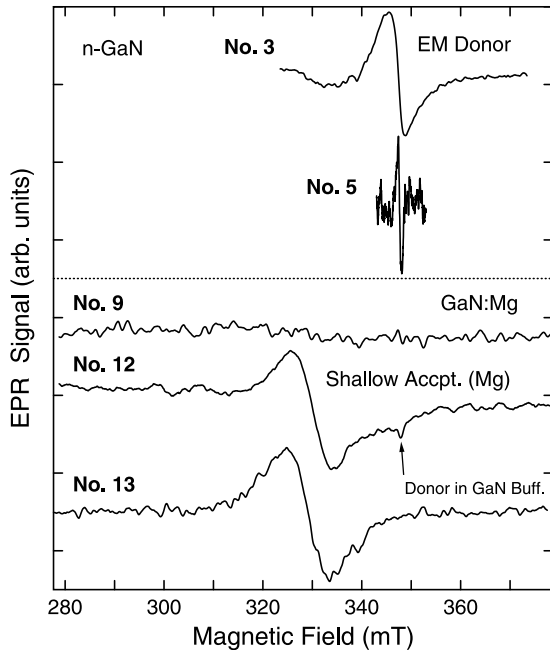[a] Estimated from growth conditions.
[b] Determined from SIMS.

Fig. 1. EPR spectra found at 9.5 GHz for n-type (as-grown and Si-doped) GaN ($\boldsymbol{B}\|c$) and Mg-doped GaN ($\boldsymbol{B}$, 30° from c).

Fig. 2. Photoluminescence spectra obtained between 1.8 and 3.4 eV from four as-grown (highly resistive and n-type) GaN layers under ~ 1 W cm^{-2} excitation (Ar^{+}-351 nm).

nuclear hyperfine interaction, it is difficult to ascertain the chemical identity of the defect(s) responsible for these signals. We note that recent donor intra-impurity for infrared transmission experiments strongly indicate that the binding energies for Si and O in GaN differ by only ~ 3 meV [22]. Even in the case of Si where the EPR lines are much sharper, the g-shifts from the free electron value of 2.0023 for shallow donors with slightly different binding energies differ by only $\sim 5\%$ [23]. Therefore, it is not expected in a III–V semiconductor that shallow donors with such small differences in binding energy could be distinguished by their g-factors. Finally, the narrow EPR line-width found for Si-doped
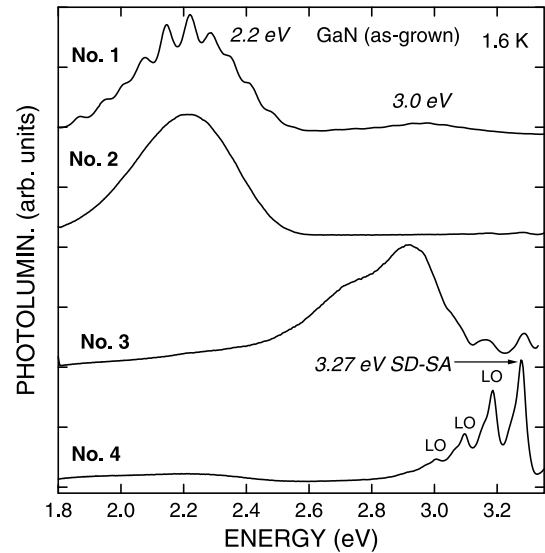
sample No. 5 is attributed to a higher concentration of donor spins compared with that, for example, in as-grown (n-type) sample No. 3. This effect arises from an averaging out of the hyperfine interaction between the delocalized spin and the host lattice nuclei [19].

The PL bands observed below 3.4 eV from samples No. 1–4 are shown in Fig. 2. All of these layers also exhibit strong excitonic recombination at low temperatures (not shown). Several emission bands of different character are found. The line at 3.27 eV and the series of LO phonon replicas at lower energies from sample No. 4 are attributed to recombination between shallow donors with $E_{\mathrm{d}} \sim 30$ meV and shallow acceptors with $E_{\mathrm{a}} \sim 200$ meV based on previous work [24]. The broad emission at ~ 3.0 eV from sample No. 1 (grown by MOCVD at

NRL) has been observed in high resistivity (HR) GaN from several other laboratories [25] and is taken as an optical signature of HR GaN. Though not typical for this growth technique, a similar emission band is found from as-grown HVPE sample No. 3. The PL most common to CVD-, MBE-, and HVPE-grown GaN is the 2.2 eV 'yellow' emission band. It is the dominant deep emission in samples No. 1,2, and 5 (not shown) and weakly observed in GaN films No. 3 and 4. In addition, samples No. 3 and 4 exhibit another broad emission band with peak energy near 1.8 eV (so-called 'red' PL), quite typical for HVPE-grown GaN [26,27].

The recombination most studied in GaN by ODMR is the 2.2 eV PL band [17,28–31]. ODMR found at 24 GHz on this emission from samples No. 2, 4, and 5 is shown in Fig. 3. Most notably, the spectra are very similar for the three different growth techniques. The sharp line with $g_{\parallel} = 1.951$ and $g_{\perp} = 1.948$ is assigned to shallow donors. The origin of the broad feature with $g_{\parallel} = 1.989$ and $g_{\perp} = 1.992$ has been the subject of much debate [2]. Most groups agree that this center is a deep defect. We first ascribed this signal to deep donors based, in part, on the small negative g-shift with respect to the free electron g-value of 2.0023 [17]. However, as discussed shortly, similar g-shifts have been recently observed for one of the external g-values (i.e. $g_{\perp}$) associated with shallow Mg acceptors in GaN [32]. Thus, we now believe that the donor or acceptor character of this deep center is an open question from a magnetic resonance viewpoint. Several groups [33,34] have proposed that Ga vacancies and/or their complexes are involved in the 2.2 eV emission. Additional magnetic resonance experiments such as ODMR on isotopically pure GaN epitaxial layers made with either ^{14}N or ^{15}N

[35] and optically detected electron-nuclear double resonance (ODENDOR) studies of the 2.2 eV emission band [36,37] have not revealed evidence that the deep defect is associated with Ga vacancies.

The ODMR found on the 3.27 eV SD-SA PL from undoped (n-type) sample No. 4 with $\boldsymbol{B}\|c$ is also shown in Fig. 3. In addition to the sharp feature ascribed to shallow donors, a broad feature with $g_{\parallel} = 2.11$ and $g_{\perp} \sim 1.98$ is found. The resonance parameters of this line are very similar to those recently observed for Mg shallow acceptors involved in similar emission from Mg-doped GaN [32]. However, SIMS measurements did not reveal evidence in this sample for Mg above the detection limit of $\sim 4 \times 10^{14}$ cm^{-3}. Other candidates for shallow acceptors in GaN are Si and C on the N sites. Recent PL work suggests that Si also introduces an acceptor level with $E_a \sim 220$ meV [38]. With [Si] $\sim 10^{17}$ cm^{-3} and [C] $\sim 10^{16}$ cm^{-3} from SIMS, this signal may be associated with SiN shallow acceptors. However, we can not rule out C being responsible for these centers.

Representative ODMR obtained at 35 GHz on the 2.2 and 3.0 eV emission bands from the high resistivity GaN film (No. 1) are shown in Fig. 4. High resistivity (HR) GaN layers are critical for high-power device applications, yet the defect(s) that give rise to this property are still not known. ODMR at 24 GHz on these bands was first reported in [39] but did not reveal two of the additional lines now obtained using a higher microwave frequency. In addition to the features assigned to shallow donors and deep defects, a line with $g_{\parallel}$, $g_{\perp} \sim 1.96$ is also observed on the 2.2 eV PL from this sample and on similar emission from HR GaN layers grown by other laboratories [40]. Based on the small difference in g-value compared with that found for EM
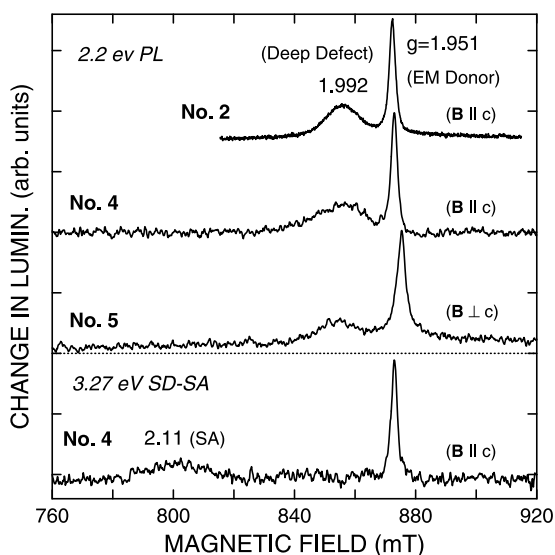

Fig. 3. ODMR found at 24 GHz on the 2.2 eV 'yellow' PL bands from CVD-, HVPE-, and MBE-grown (n-type) GaN and that detected on the 3.27 eV SD-SA PL from sample No. 4.
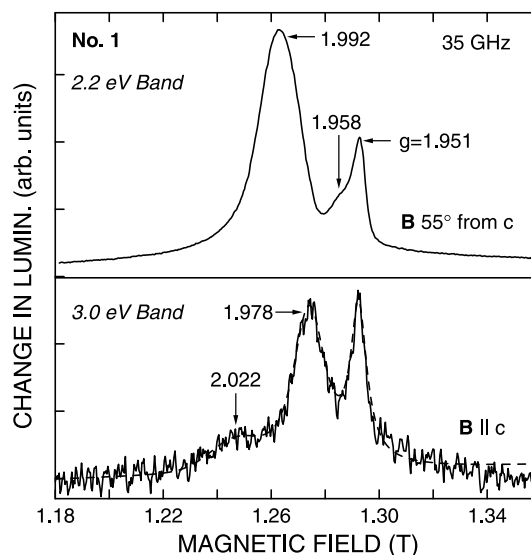

Fig. 4. ODMR spectra found at 35 GHz on the 2.2 and 3.0 eV emission bands from highly resistive GaN layer No. 1. The dashed curve is the result of a three-component lineshape fit.

shallow donors, this resonance is likely associated with shallow or quasi-shallow donors. Three features are found on the broad 3.0 eV PL band (the dashed line is the result of a three-component fit to the spectrum). In addition to the ubiquitous shallow donor resonance, an isotropic signal with $g = 1.978$ and a weaker feature with $g_{\parallel} = 2.022$ and $g_{\perp} = 2.008$ are also observed. Based on a comparison with the g-values found for shallow acceptors in GaN, the weak feature is ascribed to deep acceptors with ionization energy > 200 meV. Combined with the PL energy of ~ 3.0 eV and the observation of these deep acceptor centers, it is proposed that the feature with $g = 1.978$ is associated with donor-like centers with $E_d > 30$ meV. Overall, it is likely that one or more of the five defects revealed in the ODMR on the 2.2 and 3.0 eV PL bands play important roles in the high resistivity character of these films.

A comparison of the ODMR obtained on the 2.9 eV and 'red' PL bands from HVPE-grown sample No. 3 is shown in Fig. 5. Similar shallow donor signals with $g \sim 1.95$ are found on each band. However, different acceptor-like resonances with $g_{\parallel} = 2.019$, $g_{\perp} = 2.010$ and FWHM ~ 15 mT and $g_{\parallel}$, $g_{\perp} = 2.000$ and FWHM ~ 26 mT are observed on the 2.9 eV and 'red' PL bands, respectively. The isotropic g-tensor and broader linewidth are consistent with the deeper nature of the acceptors involved in the 'red' PL compared with those that participate in the 2.9 eV PL band. Perhaps only a coincidence, the similar magnetic resonance parameters observed for the acceptor-like resonances on the 2.9–3.0 eV PL bands from samples No. 1 and 3 suggest a common origin for this defect. In contrast to sample No. 1, however, the signal with $g = 1.978$ was not found on the 2.9 eV PL from sample No. 3.
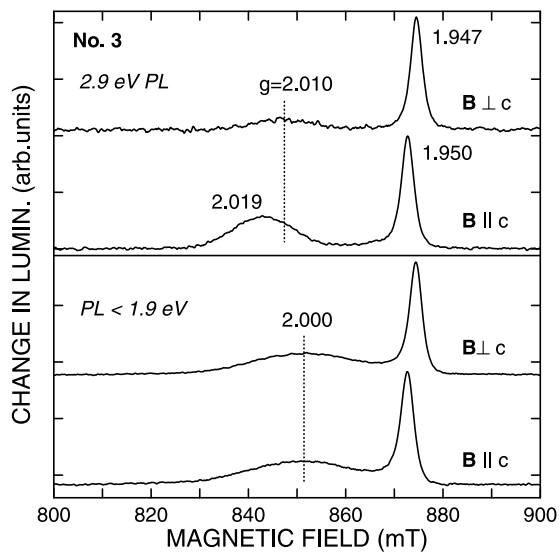
3.2. Mg-doped GaN

Mg is still the most popular dopant employed for growth of p-type GaN. Though there have been a few reports of hole concentrations $> 10^{18}$ cm^{-3}, densities in the range of low- to mid-10^{17} cm^{-3} are more typical [41]. We have attempted to address such factors such as self-compensation and/or complexing in heavily Mg-doped GaN with detailed PL and EPR/ODMR on GaN films doped with Mg from 2.5×10^{18}–5×10^{19} cm^{-3}.

EPR spectra obtained for Mg-doped GaN films No. 9, 12, and 13 are shown in the bottom half of Fig. 1. A strong line is observed from all the (p-type) conductive samples with $g_{\parallel} = 2.071$–2.112 and $g_{\perp} = 1.994$–2.032. No signal was found from samples No. 9 and 10, consistent with the highly resistive character as revealed by the transport measurements. The EPR is assigned to (neutral) shallow Mg acceptors based on the similarity of the spin densities with the concentrations of electronically-active Mg acceptors determined by temperature-dependent Hall effect and the total [Mg] as revealed by SIMS or estimated from the growth conditions. It is puzzling that although the g-anisotropy ($\Delta g \equiv g_{\parallel} - g_{\perp} \sim 0.1$) is the largest observed for any acceptor in GaN, the degree of anisotropy is much smaller than that expected (i.e. $g_{\parallel} \sim 2$–4, $g_{\perp} \sim 0$) for shallow acceptors from effective mass theory [42]. Regardless, these resonance parameters serve as an

Fig. 5. ODMR obtained on the 2.9 eV PL band and on the emission less than 1.9 eV ('red' PL) from HVPE-grown GaN sample No. 3. The dotted lines indicate the positions of the broad features with **B** ⊥ c.
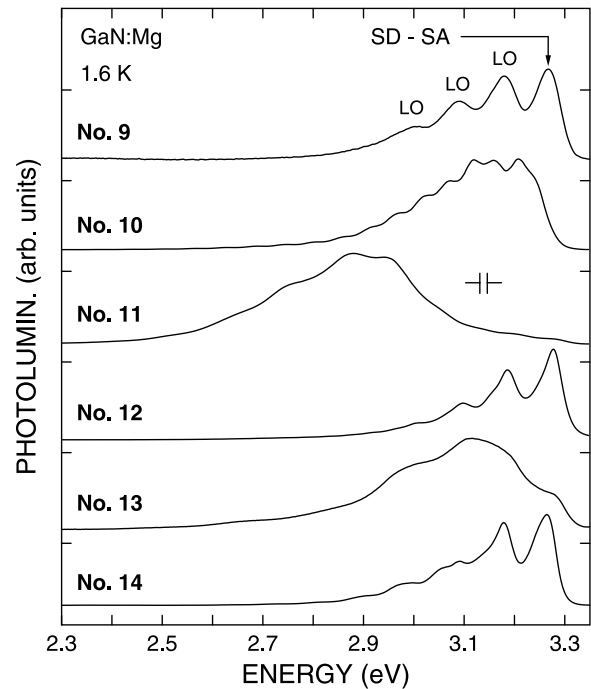

Fig. 6. PL spectra obtained in the 'blue' spectral region from six Mg-doped GaN layers grown by CVD and MBE. The structure on the broad emission from samples Nos. 10, 11, and 13 is due to Fabry–Perot interference effects.

important benchmark for comparison with the ODMR obtained on the PL from these samples discussed below.

The dominant PL bands observed from the six Mg-doped GaN layers are shown in Fig. 6. These are often referred to as the 'blue' emission bands. The PL at ~ 3.27 eV and the series of LO phonon replicas at lower energy from samples No. 9, 12, and 14 are assigned to recombination between shallow donors ($E_d \sim 30$ meV) and shallow Mg acceptors ($E_a \sim 230$ meV) based on previous work [43]. Broad emission bands with peak energy between 2.8 and 3.2 eV are observed from samples No. 10,11, and 13. Their origin has been a subject of high interest. One group has proposed that the broad PL near 3.2 eV still involves shallow donors and shallow acceptors but in the presence of large potential fluctuations that arise from a random distribution of positively- and negatively-charged impurities [44]. Several groups [6,44–46] have suggested that the broad PL near 2.8 eV is due to recombination between deep (compensating) donors and shallow Mg acceptors. In addition, several of these samples and those reported by others [6,18] also exhibit a broad emission band with peak energy near 1.7 eV (not shown).

The ODMR on the 3.27 eV SD-SA recombination from MBE-grown sample No. 14 is shown in Fig. 7. The sharp line (labeled EM) with $g_{\parallel}$, $g_{\perp} \sim 1.95$ is again ascribed to shallow donors. The broad signal (labeled Mg) is more anisotropic with $g_{\parallel} = 2.108$ and $g_{\perp} = 1.98$. This feature is assigned to shallow Mg acceptors based

Fig. 8. ODMR found on the 'blue' emission bands from six Mg-doped GaN layers with **B**||*c*. The feature with $g \sim 2.1$ is attributed to Mg shallow acceptors.
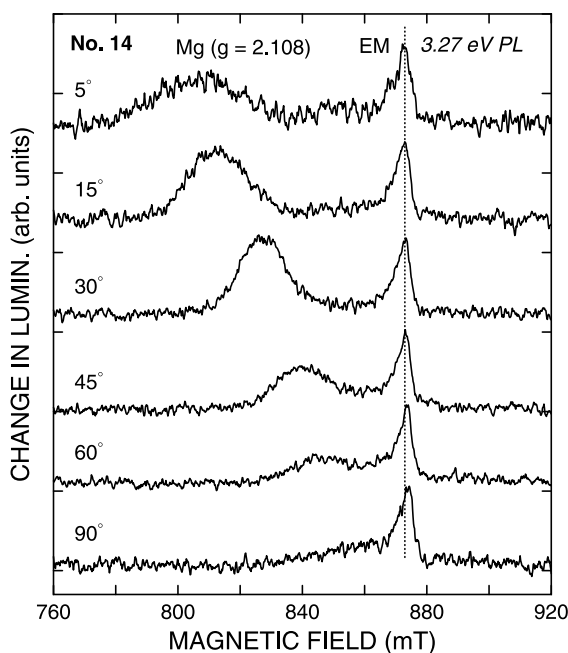
Fig. 7. ODMR spectra obtained on the 3.27 eV shallow donor-shallow acceptor PL from Mg-doped GaN sample No. 14. The dotted line indicates the position of the EM donor resonance with **B** nearly parallel to the *c*-axis.

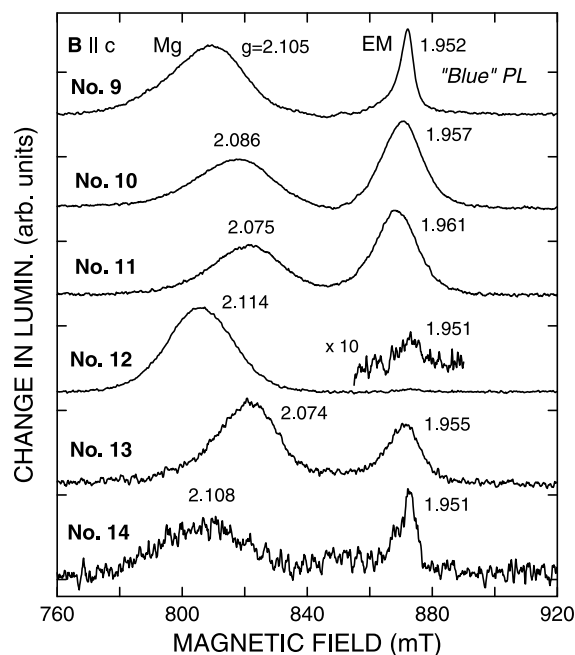on the similarity of the g-values with those found from EPR and the identical spectral dependencies of the ODMR and PL [32].

ODMR spectra obtained on the 'blue' emission bands from all six Mg-doped GaN layers with **B**||*c* are shown in Fig. 8 (similar ODMR has been reported by others [28,47] on the broad 2.8–3.2 eV PL). Two luminescence-increasing signals are found in each case. The first feature is described by $g_{\parallel} = 2.074-2.108$ and $g_{\perp} = 1.98-2.006$ and is assigned to shallow Mg acceptors based on the similarity with the EPR results. The small variation observed among these samples in the Mg EPR/ODMR g-tensors may be associated with the nature of the local environment at the Mg sites. For example, the g-values are likely influenced by the presence of local electric fields associated with nearby grain boundaries or those associated with potential fluctuations that have been proposed to play a role in the recombination from highly doped and compensated GaN [44].

The second signal is characterized by $g_{\parallel} = 1.951-1.961$ and $g_{\perp} = 1.948-1.957$ and are attributed to shallow donors (the small intensity of the donor signal observed on the 3.27 eV PL from sample No. 12 is not understood at this time). Most notably, no clear evidence is found for deep donors within a simple model that the two features (Mg and EM) observed from ODMR on the broad 2.8–3.2 eV PL bands are associated with the recombining centers. However, we suggest that evidence for the existence of deep donors in several of these samples is found from ODMR on the PL < 1.9 eV [48]. In addition to the same Mg-related

ODMR feature as observed on the 'blue' PL bands, an isotropic line with $g = 2.003 \pm 0.002$ and FWHM ~ 15–20 mT is also found on this near-IR PL (though the g-values are very similar, this resonance is much broader than the MM1 signal observed on emission less than 1.9 eV from Mg-doped GaN reported in [18]). This feature is attributed to deep donors with an energy level near mid-gap based on the PL energy and the known binding energy of shallow Mg acceptors.

3.3. Be-doped GaN

Attempts made during the last several years to produce p-type GaN via Be-doping have met with limited success. In addition to the normal substitution of Be on the host Ga lattice sites, it has been suggested that self-compensating (donor-like) Be interstitials (Be_i) and Be-related deep acceptor complexes also likely form in Be-doped GaN [49]. Such defects will certainly impact the doping efficiency and make it quite problematic to achieve high hole concentrations.

The three Be-doped GaN layers (Nos. 6–8) investigated in this work were highly resistive from two-point probe measurements. The absence of a measurable EPR signal (not shown) in the dark that could be associated with uncompensated (neutral) shallow Be acceptors is consistent with these transport results. The best evidence perhaps for the existence of shallow Be acceptors in these films is from the low-temperature PL studies. The near bandgap and deep emission bands observed from samples Nos. 6–8 are shown in Fig. 9. The line at 3.38 eV and the series of LO phonon replicas are assigned to recombination between shallow donors ($E_d \sim 30$ meV) and shallow Be acceptors with $E_a \sim 100$ meV [50],
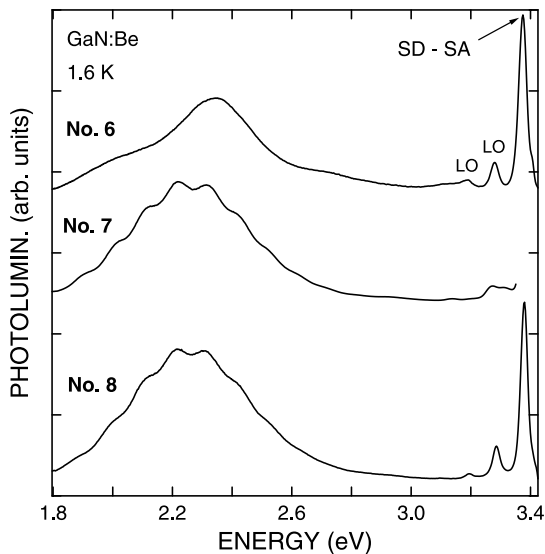

Fig. 9. Near band-edge and deep emission from three Be-doped GaN films. The sharp line at ~ 3.38 eV is assigned to recombination between shallow donors and Be shallow acceptors with $E_b \sim 100$ meV.
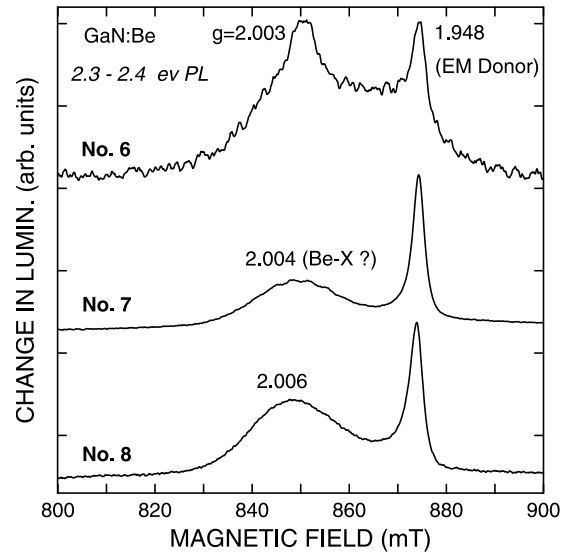

Fig. 10. ODMR found on the 2.3–2.4 eV PL bands from Be-doped GaN with $\boldsymbol{B} \perp c$. The broad feature with $g = 2.004 \pm 0.002$ is likely associated with a Be-related (deep) acceptor complex as suggested in [49].

roughly half the binding energy found for shallow Mg acceptors in GaN. In addition, all three samples exhibit a broad emission band with peak energy near 2.35 eV.

It is puzzling that, to date, ODMR has not been found on the Be-related 3.38 eV SD-SA PL. However, as first reported for sample No. 6 in [50], strong ODMR is observed on the deep 2.3–2.4 eV PL bands as shown in Fig. 10. Two resonances are clearly resolved on this emission. In addition to the EM shallow donor resonance, an isotropic feature with $g = 2.004 \pm 0.002$ is found and tentatively ascribed to deep acceptors based on the magnetic resonance parameters. Its observation in all three MBE samples (grown by two different laboratories) and on similar emission from a Be-doped bulk GaN crystal grown by a high pressure–high temperature process [51] strongly suggests that it is associated with a Be-related defect. One group has proposed that this deep defect is a Ga vacancy—Be_i complex from positron annihilation and (Mg + Be) co-doping studies [49]. The present ODMR results do not exclude this possibility.

3.4. InGaN LEDs and heterostructures

There has been much activity during the last five years to obtain a better understanding of the mechanism(s) and dynamics of recombination in the 20–30 Å-thick $In_{1-x}Ga_xN$ quantum wells that are employed as active layers in visible and near UV light-emitting-diodes (LEDs) and laser diodes (LDs) [13]. Several groups [52] have proposed that the strong recombination arises from the high degree of electron and hole localization in In-rich 'quantum dots' with diameters of ~ 2–5 nm as

revealed from TEM measurements. In addition, piezo-electric fields (both strain-induced and spontaneous) are also thought to strongly influence the optical processes in these thin layers [53].

We have extended our earlier ODMR investigation of the recombination from green and extra-blue LEDs [3] to devices that emit at shorter ('violet') and longer ('amber') wavelengths. The four samples were diced from ~ 30 Å-thick SQW InGaN device wafers prior to the etching and metalization steps. The PL at 1.6 K from the 4 LED structures under low photoexcitation (~ 20 mW cm^{-2}) is shown in Fig. 11. The emission energies of 2.0–3.2 eV are very similar to those observed from electroluminescence of similar (fully processed) InGaN LEDs [13].

ODMR obtained at 24 GHz on the PL from the four LEDs with $\boldsymbol{B}\|c$ is shown in Fig. 12. As observed for the green and extra-blue LEDs [3], two strong luminescence-increasing signals (labeled E and H) are also found from the violet and amber LEDs. We again ascribe the strength of these signals (i.e. ΔPL/PL ~ 1–3%) to significant charge separation under these low photo-excitation conditions. Indeed, long lifetimes of the order of 0.2 ms are deduced from microwave modulation frequency studies [4]. The external g-values of the two signals for all four samples are summarized in Table 2.

The line E is assigned to electrons in the InGaN SQWs as argued in [3]. Most notably, it appears that the electron g-values depend on the In mole fraction and effects due to quantum confinement and/or the nature of the strain in the layers. In particular, a monotonic decrease of the g-values with increasing In mole fraction from the shallow donor/conduction electron g-value of

Fig. 12. ODMR spectra found at 24 GHz from the four InGaN LEDs with $\boldsymbol{B}\|c$. The features labeled E and H are assigned to the recombining electrons and holes, respectively, in the InGaN single quantum wells.

Table 2
Summary of magnetic resonance parameters from ODMR of NICHIA LEDs and (undoped) 30 Å In$_{0.3}$Ga$_{0.7}$N/GaN heterostructure

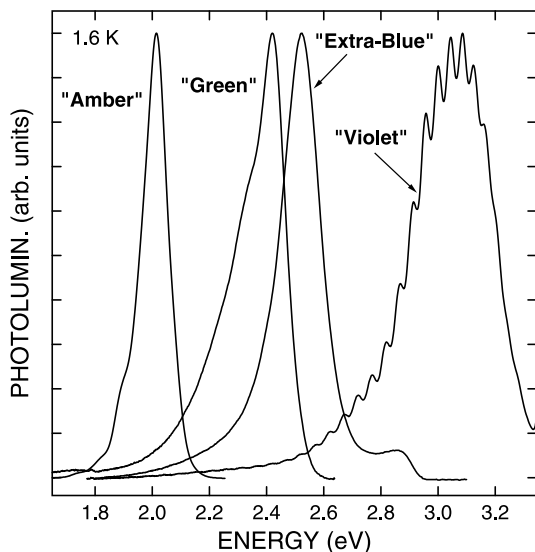| Sample	PL Energy (eV)	Electron	Hole
Violet LED	3.06	$g_{\|} = 1.953$, $g_{\perp} = 1.949$	$g_{\|} = 2.038$, $g_{\perp} = 2.010$
Extra-Blue LED	2.52	$g_{\|} = 1.947$, $g_{\perp} = 1.956$	$g_{\|} = 2.066$, $g_{\perp} = 2.023$
Green LED	2.42	$g_{\|} = 1.934$, $g_{\perp} = 1.928$	$g_{\|} = 2.08$, $g_{\perp} = 1.996$
Amber LED	2.02	$g_{\|} = 1.926$, $g_{\perp} = 1.918$	$g_{\|} = 2.217$, $g_{\perp} = 1.983$
30 Å In$_{0.3}$ Ga$_{0.7}$N/GaN	2.17	$g_{\|} = 1.940$, $g_{\perp} = 1.937$	$g_{\|} = 2.14$, $g_{\perp} = 1.98$

Fig. 11. PL spectra obtained from four NICHIA InGaN LEDs at 1.6 K under low photoexcitation (~ 20 mW cm^{-2}). Excitation wavelengths were 458 nm for the amber and green LEDs and 364 nm for the extra-blue and violet LEDs. The structure on the emission from the 'violet' LED is due to Fabry–Perot interference effects.
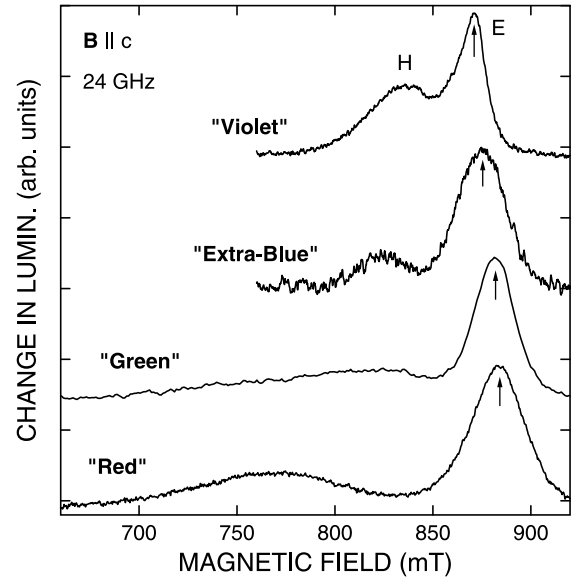
1.95 in GaN is expected from a five band quasi-cubic $\boldsymbol{k}\cdot\boldsymbol{p}$ calculation [3]. Evidence for this behavior is seen from a comparison of the electron $g_{\|}$-values in the extra-blue, green, and amber LEDs assuming that the average In composition is progressively higher in those samples. However, it has been proposed recently from high-resolution TEM experiments [54] that the In composition in blue and green NICHIA LEDs are quite similar (such measurements have not been reported for the amber and violet LEDs). Instead, a smaller InGaN well width in the blue LED, compared with that found for the green LED in the same TEM study, is suggested to account for the higher emission energy. Based on other work [55,56], such quantum confinement effects can also explain the changes observed in the electron g-values of

the green and extra-blue LEDs. This is perhaps best demonstrated from the ODMR of the violet LED where the electron $g_{\parallel}$-value is greater than 1.95. This result indicates that alloy effects alone can not be used to predict conduction electron g-values in InGaN quantum wells.

The g-tensors for line H are very similar to those found from EPR/ODMR of Mg-doped GaN samples No. 9–14. Thus, it was proposed earlier [3] that this feature may be associated with Mg acceptors in the p-AlGaN layer adjacent to the InGaN SQWs. In order to test this model, ODMR was done on PL ($\sim$2.17 eV) from a simple (undoped) 30 Å-thick $In_{0.3}Ga_{0.7}N$/GaN heterostructure. Most notably, similar ODMR was found on this emission (see Table 2). Thus, from this comparison, line H in the NICHIA LEDs is attributed to holes in the optically-active InGaN SQWs. The variation in hole g-tensors is again likely due to a combination of effects from alloy composition, quantum confinement, and/or strain.

Two models are considered that can account for the recombination in the InGaN LEDs and heterostructures under low photoexcitation conditions based on the charge separation typically required for observation of strong ODMR. In the first (Fig. 13a), the electrons and holes are localized at different potential minima in the $x-y$ planes that can arise from In mole fraction

inhomogeneities, well-width variations, and/or strain fluctuations. In the second (Fig. 13b), the electrons and holes are spatially separated along the growth direction from the large strain-induced piezoelectric fields ($\sim$ mid 10^5–10^6 V cm^{-1}). This model is not ruled out but a simple effective-mass calculation indicates significant overlap of the electron and hole wave functions in a 30 Å $In_{0.3}Ga_{0.7}N$ SQW under a field of 10^6 V cm^{-1}. One would expect much shorter lifetimes ($\ll$100 ns as measured by others under high photoexcitation or current injection conditions) and weak ODMR for the microwave powers employed in this work.

4. Summary

EPR and ODMR have been performed on a set of undoped (highly resistive and n-type) and intentionally doped (Si, Mg, or Be) GaN heteroepitaxial layers grown by MOCVD, MBE, and HVPE. Many of the same residual and dopant-related defects are observed in these samples. In some cases, different defects are found to be involved in emission bands that appear at first inspection to be of similar character based on their peak energy and linewidth. Similar ODMR was found on emission from state-of-the-art violet and amber InGaN SQW LEDs as first reported for green and extra-blue LEDs [3]. A comparison with the ODMR on a 30 Å-thick InGaN/GaN heterostructure suggests that under low photoexcitation the recombining electrons and holes are spatially separated in the InGaN layers at different potential minima in the $x-y$ planes or along the growth direction from the large strain-induced piezoelectric fields.

(a)

CB

VB

QW (x,y)

(b)
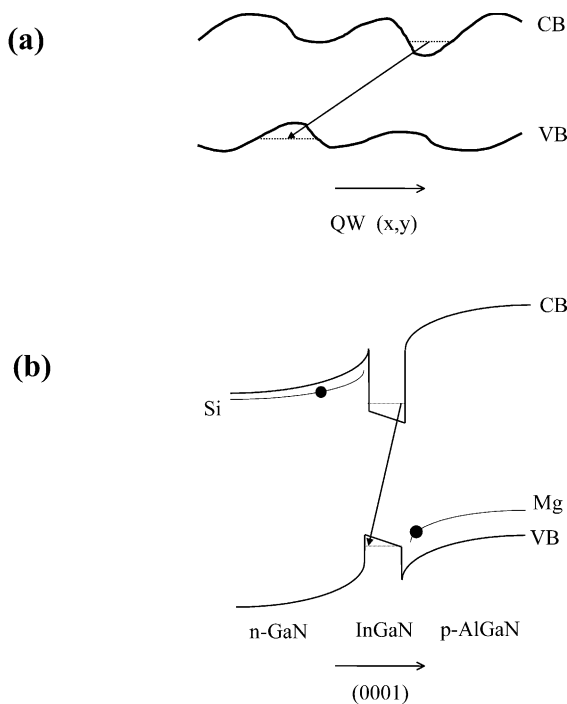
CB

Si

Mg

VB

n-GaN   InGaN   p-AlGaN

(0001)

Fig. 13. Recombination models for InGaN LEDs under low photoexcitation. Electron and hole are spatially separated due to: (a) localization at different potential minima in the $x-y$ plane; (b) the large piezoelectric field across the InGaN SQW.

References

[1] For a review, see W.E. Carlos, in: J.H. Edgar, Toby Strite, I. Akasaki, H. Amano (Eds.), Properties of GaN, INSPEC, London, 1999, pp. 104–114.

[2] For a review, see B.K. Meyer, in: Semiconductors and Semimetals, vol. 57 1999 pp. 371–406.

[3] E.R. Glaser, T.A. Kennedy, W.E. Carlos, P.P. Ruden, S. Nakamura, Appl. Phys. Lett. 73 (1998) 3123.

[4] W.E. Carlos, E.R. Glaser, T.A. Kennedy, S. Nakamura, J. Electron. Mater. 28 (1999) 250 (and references therein).

[5] A.E. Wickenden, D.K. Gaskill, D.D. Koleske, K. Doverspike, D.S. Simons, P.H. Chi, Mat. Res. Soc. Symp. Proc. 395 (1996) 679.

[6] U. Kaufmann, M. Kunzer, H. Obloh, M. Maier, Ch. Manz, A. Ramakrishnan, B. Santic, Phys. Rev. B 59 (1999) 5561.

[7] H. Kozodoy, S.P. Xing, U.K. DenBaars, A. Mishra, R. Saxler, S.E.lhamri Perrin, W.C. Mitchel, J. Appl. Phys. 87 (2000) 1832.

[8] I.P. Smorchokova, E. Haus, B. Heying, P. Kozodoy, P. Fini, J.P. Ibbetson, S. Keller, S.P. DenBaars, J.S. Speck, U.K. Mishra, Appl. Phys. Lett. 76 (2000) 718.

[9] J.E. Van Nostrand, J. Solomon, A. Saxler, Q.-H. Xie, D.C. Reynolds, D.C. Look, J. Appl. Phys. 87 (2000) 8766.

[10] M.A. Sánchez-García, E. Calleja, E. Monroy, D. Basak, E. Muñoz, C. Villar, R. Beresford, J. Crystal Growth 183 (1998) 23.

[11] T.H. Myers, M.R. Millecchia, A.J. Ptak, K.S. Ziemer, C.D. Stinespring, J. Vac. Sci. Technol. B 17 (1999) 1654.

[12] R.J. Molnar, K.B. Nichols, P. Makai, E.R. Brown, I. Melngailis, Mat. Res. Soc. Symp. Proc. 378 (1995) 479.

[13] See, for example, S. Nakamura, G. Fasol, in: The Blue Laser Diode, Springer-Verlag, Berlin, 1997.

[14] J.A. Freitas, Jr, K. Doverspike, A.E. Wickenden, Mat. Res. Soc. Symp. Proc. 395 (1996) 485.

[15] J.A. Freitas, Jr, T.A. Kennedy, E.R. Glaser, W.E. Carlos, Solid-State Electron. 41 (1997) 185.

[16] G.C. Braga, J.A. Freitas, Jr, P.B. Klein, R.L. Henry, A.E. Wickenden, D.D. Koleske, unpublished.

[17] E.R. Glaser, T.A. Kennedy, K. Doverspike, L.B. Rowland, D.K. Gaskill, J.A. Freitas, Jr, M. Asif Khan, D.T. Olson, J.N. Kuznia, D.K. Wickenden, Phys. Rev. B 51 (1995) 13326.

[18] M.W. Bayerl, M.S. Brandt, O. Ambacher, M. Stutzmann, E.R. Glaser, R.L. Henry, A.E. Wickenden, D.D. Koleske, T. Suski, I. Grzegory, S. Porowski, Phys. Rev. B 63 (2001) 125023.

[19] W.E. Carlos, J.A. Freitas, M. Asif Khan, D.T. Olson, J.N. Kuznia, Phys. Rev. B 48 (1993) 17878 (and references therein).

[20] N.M. Reinacher, H. Angerer, O. Ambacher, M.S. Brandt, M. Stutzmann, Mat. Res. Soc. Symp. Proc. 449 (1997) 579.

[21] M. Palczewska, B. Suchanek, R. Dwilinski, K. Pakula, A. Wagner, M. Kaminska, MRS Internet J. Nitride Semicond. Res. 3 (1998) 45.

[22] W.J. Moore, J.A. Freitas, Jr, G.C.B. Braga, R.J. Molnar, S.K. Lee, K.Y. Lee, I.J. Song, Appl. Phys. Lett. 79 (2001) 2570.

[23] G. Feher, Phys. Rev. 114 (1959) 1219.

[24] R. Dingle, M. Ilegems, Solid State Commun. 9 (1971) 175.

[25] See, for example, B. Kim, I. Kuskovsky, I.P. Herman, D. Li, G.F. Neumark, J. Appl. Phys. 86 (1999) 2034.

[26] W. Götz, L.T. Romano, B.S. Krusor, N.M. Johnson, R.J. Molnar, Appl. Phys. Lett. 69 (1996) 242.

[27] S.J. Rhee, S. Kim, E.E. Reuter, S.G. Bishop, R.J. Molnar, Appl. Phys. Lett. 73 (1998) 2636.

[28] U. Kaufmann, M. Kunzer, C. Merz, I. Akasaki, H. Amano, Mat. Res. Soc. Symp. Proc. 395 (1996) 633 (and references therein).

[29] D.H. Hofmann, D. Kovalev, G. Steude, B.K. Meyer, A. Hofmann, L. Eckey, R. Heitz, T. Detchprohm, H. Amano, I. Akasaki, Phys. Rev. B 52 (1995) 16702.

[30] F.K. Koschnick, K. Michael, J.-M. Spaeth, B. Beaumont, P. Gibart, Phys. Rev. B 54 (1996) R11042.

[31] P.W. Mason, G.D. Watkins, A. Dornen, Mat. Res. Soc. Symp. Proc. 449 (1997) 793.

[32] E.R. Glaser, T.A. Kennedy, J.A. Freitas, Jr, B.V. Shanabrook, A.E. Wickenden, D.D. Koleske, R.L. Henry, H. Obloh, Physica B 273–274 (1999) 58.

[33] J. Neugebauer, C. Van de Walle, Appl. Phys. Lett. 69 (1996) 503.

[34] K. Saarinen, et al., Phys. Rev. Lett. 79 (1997) 3030.

[35] M.W. Bayerl, N.M. Reinacher, H. Angerer, O. Ambacher, M.S. Brandt, M. Stutzmann, J. Appl. Phys. 88 (2000) 3249.

[36] E.R. Glaser, T.A. Kennedy, W.E. Carlos, J.A. Freitas, Jr, A.E. Wickenden, D.D. Koleske, Phys. Rev. B 57 (1998) 8957.

[37] F.K. Koschnick, K. Michael, J.-M. Spaeth, B. Beaumont, P. Gibart, E. Calleja, E. Munoz, J. Electron. Mater. 29 (2000) 1351.

[38] J. Jayapalan, B.J. Skromme, R.P. Vaudo, V.M. Phanse, Appl. Phys. Lett. 73 (1998) 1188.

[39] E.R. Glaser, T.A. Kennedy, A.E. Wickenden, D.D. Koleske, J.A. Freitas, Jr, Mat. Res. Soc. Symp. Proc. 449 (1997) 543.

[40] E.R. Glaser, unpublished.

[41] See, for example, D.P. Bour, H.F. Chung, W. Götz, L. Romano, B.S. Krusor, D. Hofstetter, N.M. Johnson, M.G. Craford, R.D. Bringans, Mat. Res. Soc. Symp. Proc. 449 (1997) 507.

[42] A.V. Malyshev, I.A. Merkulov, A.V. Rodina, Phys. Solid State 40 (1998) 917.

[43] M. Ilegems, R. Dingle, J. Appl. Phys. 44 (1973) 4234.

[44] M.A. Reshchikov, G.C. Yi, B.W. Wessels, Phys. Rev. B 59 (1999) 13176.

[45] S.G. Lee, K.J. Chang, Semicond. Sci. Technol. 14 (1999) 138.

[46] H. Teisseyre, T. Suski, P. Perlin, I. Grzegory, M. Leszczynski, M. Bockowski, S. Porowski, J.A. Freitas, Jr, R.L. Henry, A.E. Wickenden, D.D. Koleske, Phys. Rev. B 62 (2000) 10151.

[47] F.K. Koschnick, K. Michael, J.-M. Spaeth, B. Beaumont, P. Gibart, J. Off, A. Sohmer, F. Scholz, J. Crystal Growth 189–190 (1998) 561.

[48] E.R. Glaser, G.C.B. Braga, W.E. Carlos, J.A. Freitas, Jr, R.L. Henry, D.D. Koleske, B.V. Shanabrook, A.E. Wickenden, W.J. Moore, H. Obloh, P. Kozodoy, S.P. DenBaars, U.K. Mishra, Phys. Rev. B 65 (2002) in press.

[49] E. Calleja, M.A. Sánchez-García, F. Calle, F.B. Naranjo, E. Muñoz, U. Kahn, K. Ploog, J. Sánchez, J.M. Calleja, K. Saarinen, J. Oila, P. Hautojärvi, Mater. Sci. Eng. B82 (2001) 2.

[50] F.J. Sánchez, F. Calle, M.A. Sánchez-García, E. Calleja, E. Muñoz, C.H. Molloy, D.J. Somerford, F.K. Koschnick, K. Michael, J.-M. Spaeth, MRS Internet J. Nitride Semicond. 3 (1998) 19.

[51] M.W. Bayerl, M.S. Brandt, M. Stutzmann, T. Suski, I. Grzegory, S. Porowski, unpublished.

[52] See, for example, K.P. O'Donnell, R.W. Martin, P.G. Middleton, Phys. Rev. Lett. 82 (1999) 237.

[53] See, for example, P. Perlin, C. Kisielowski, V. Iota, B.A. Weinstein, L. Mattos, N.A. Shapiro, J. Kruger, E.R. Weber, Appl. Phys. Lett. 73 (1998) 2778.

[54] N.A. Shapiro, P. Perlin, C. Kisielowski, L.S. Mattos, J.W. Yang, E.R. Weber, MRS Internet J. Nitride Semicond. Res. 5 (2000) 1.

[55] See, for example, E.L. Ivchenko, A.A. Kiselev, Sov. Phys. Semicond. 26 (1992) 827.

[56] A. Malinowski, R.T. Harley, Phys. Rev. B 62 (2000) 2051.